ARTICLES

Experimental and Simulation Studies of the Dielectric Relaxation of 2,2-Bis[4-(2-hydroxyethoxy)phenyl]propane Diacetate (DDA) in the Liquid State

Enrique Saiz[†] and Evaristo Riande*

Departamento de Química Física, Universidad de Alcalá, 28871-Alcalá de Henares, Madrid, Spain, and Instituto de Ciencia y Tecnología de Polímeros (CSIC), 28006-Madrid, Spain

Received: January 6, 2000; In Final Form: March 28, 2000

Molecular dynamic simulations of the time dipole correlation function $g(t)$ were performed, at several temperatures, for both an isolated molecule of 2,2-bis[4-(2-hydroxyethoxy)phenyl]propane diacetate (DDA) and a canonical ensemble of these molecules contained within a cubic box with periodic boundary conditions. To perform the simulations in a reasonable computing time, the calculations were carried out at temperatures well above the glass-transition temperature. Fitting of the relaxation response in the time domain to the KWW equation $g(t) = \exp[-(t/\tau^*)^{\bar{\beta}}]$ is good for rather low values of the stretch exponent. The nature of the simulated relaxations is discussed.

Introduction

The prediction of the relaxation behavior of supercooled liquids is a central and still unresolved issue in condensed matter physics.[1−6] In general, the relaxation response of the condensed matter in the equilibrium liquid range, and into the moderately supercooled regime, to a perturbation field, is a single absorption, named $\alpha\beta$ relaxation, which with declining temperature can split into two processes, one slow and another fast called α and β relaxations, respectively.[2] As the temperature comes near the glass transition temperature, the mean-relaxation time associated with the relaxation response experiences a dramatic increase, described by the Vogel−Fulcher−Tammann−Hesse (VFTH) empirical equation[7−9]

$$\tau = \tau_0 \exp\left(\frac{m}{T - T_0}\right) \tag{1}$$

where τ_0 is of the order of picoseconds. As long as the relaxation time τ is lower than the time scale of the experiment, τ_{exp}, supercooled liquids remain in a state of quasi-equilibrium. However, as T decreases, a temperature can be reached at which $\tau > \tau_{exp}$, however large τ_{exp} is. At this temperature, called the glass transition temperature or T_g, the system falls out of equilibrium, and the transition from the supercooled state to the glassy state occurs. The α relaxation becomes frozen at T_g, but the β process remains operative in the glassy state.

Götze and co-workers[10] have described a mode-coupling theory (MCT) for relaxation of supercooled liquids that leads to a behavior at long times that resembles the Kohlrausch−Williams−Watts (KWW)[11] decay function and also leads to predictions of bifurcation in behavior at a temperature T_c, well above T_g, and to a loss of the ergodic behavior of the relaxation process. A model has recently been formulated[12] that not only describes the splitting of the $\alpha\beta$ relaxation to the α and β processes but also the glass transition temperature and the effects of the thermal history in this transition, in a unified way. However, neither this model nor the MCT relate the relaxation behavior of supercooled liquids to their chemical structure. Molecular dynamics may be an important tool to accomplish this task. Thus the normalized relaxation response function to an electric field, also called time dipole correlation function, can be written in molecular terms as[13]

$$g(t) = \frac{\langle \mu_i(0)\cdot\mu_i(t)\rangle + \sum_{i\neq j}\langle \mu_i(0)\cdot\mu_j(t)\rangle}{\langle \mu_i(0)^2\rangle + \sum_{i\neq j}\langle \mu_i(0)\cdot\mu_j(0)\rangle} \tag{2}$$

where $\mu_j(t)$ is the dipole moment of the molecule j at time t. In principle, it is possible to evaluate in a quantitative way the evolution with time of the trajectories of the dipoles of the particles in the configurational space as a function of the chemical structure and to obtain from the trajectories the time dipole correlation function $g(t)$. A shortcoming of this approach, however, is that to obtain these trajectories in a reasonable computing time requires utilization of temperatures far above the glass transition temperature.

In this paper we study the equilibrium dielectric properties of 2,2-bis[4-(2-hydroxyethoxy)phenyl]propane diacetate (DAA), expressed in terms of its mean-square dipole moment. The value of this quantity is calculated by molecular dynamics and compared with that experimentally obtained. In addition the time dipole correlation function is simulated at several temperatures from which the mean-relaxation times associated with the responses are compared with those determined from the experimental relaxation spectra of DDA. The nature of the

* Instituto de Ciencia y Tecnología de Polímeros (CSIC).
† Universidad de Alcalá.

10.1021/jp000076h CCC: $19.00
Published on Web 05/27/2000

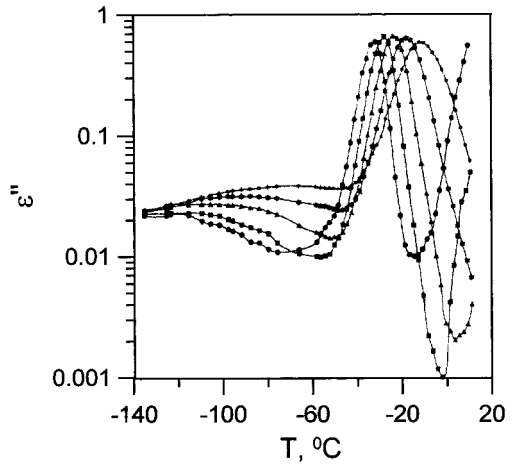

Figure 1. Isochrones showing the temperature dependence of the dielectric loss of an isolated molecule of 2,2-bis[4-(2-hydroxyethoxy)-phenyl]propane diacetate (DDA) at several frequencies: (●) 0.003; (■) 0.03; (▲) 0.3;(☆) 3; (★) 30 kHz.

relaxation responses obtained by molecular dyanamics are discussed in the light of the heterogeneous dissipation coupling (HDC) model recently formulated.[12]

Experimental Part

2,2-Bis[4-(2-hydroxyethoxy)phenyl]propane, purified by crystallization in methanol, was refluxed with glacial acetic acid. The 2,2-bis[4-(2-hydroxyethoxy)phenyl]propane diacetate formed was extracted from the reaction medium with diethyl ether, dried over calcium chloride, and purified by vacuum distillation. The glass transition temperature of DDA, measured at a heating rate of 5 °C/min with a DSC-4 Perkin-Elmer calorimeter, was −25 °C.

The complex dielectric permittivity of DDA in the bulk was measured with a Du Pont DEA 2970 apparatus, in the frequency interval 0.003−30 kHz and temperature range −80−20 °C. The temperature dependence of the dielectric loss, shown in Figure 1, exhibits a weak subglass absorption followed by an ostensible peak associated with the glass−liquid transition.[14]

The static dielectric permittivity, ϵ, of solutions of DDA in benzene was measured at 30 °C with a capacitance bridge (General Radio, type 1620 A). The increment of the index of refraction of the solutions with respect to that of the solvent ($\Delta n = n - n_1$) was determined with a differential refractometer (Chromatix, Inc).

The mean-square dipole moment, $\langle \mu^2 \rangle$, of Dianol 22 diacetate was obtained by means of the equation of Guggenheim and Smith[15]

$$\langle \mu^2 \rangle = \frac{27 k_B T M}{4\pi\rho N_A (\epsilon_1 + 2)^2}\left(\frac{d\epsilon}{dw} - 2n_1\frac{dn}{dw}\right) \qquad (3)$$

where M is the molecular weight of the solute, k_B and N_A are respectively the Boltzmann constant and Avogadro's number, ρ and ϵ_1 are respectively the density and the dielectric permittivity of the solvent, and w is the weight fraction of DDA in the solution. The values of $d\epsilon/dw$ and $2n_1 dn/dw$, which are proportional respectively to the total and electronic polarizations, are 2.14 and 0.14 at 30 °C, respectively. These results in conjunction with eq 3 give 7.6 ± 0.3 D^2 for the mean-square dipole moment of DDA.

MD Simulations Analysis

Figure 2 shows a sketch of the DDA molecule in its planar all-trans conformation, in which all the rotational angles will be assumed to have values $\phi = 180°$. Molecular dynamics (MD) simulations were performed according to standard procedures[16] with the DL_POLY package[17] employing the AMBER force field.[18−20] A time step $\delta = 1$ fs (i.e., 1^{-15} s) was used for the integration cycle. Partial charges were assigned to every atom of the sample by means of the AMPAC program and the PM3 procedure.[21] These charges were employed both to evaluate the Coulombic term of the potential energy and to compute the dipole moment of every conformation adopted by the molecules of the system along the MD trajectories. The temperature of the sample was controlled by scaling the atomic velocities after each integration cycle employing a Nose-Hoover thermostat[16,17] with a coupling factor of 1000 fs in order to allow relatively high thermal fluctuations that will facilitate the passage over energy barriers.[22]

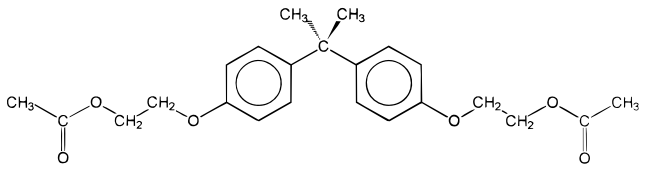

Figure 2. Rough sketch of 2,2-bis[4-(2-hydroxyethoxy)phenyl]propane diacetate (DDA) in its planar all-trans conformation, in which all the rotational angles will be assumed to have values $\phi = 180°$.

Two different molecular systems were employed for the present calculations. The first one consisted of a single molecule of DDA, which was assumed to stand alone in vacuo, while the second one was a canonical ensemble (i.e., constant *T, V, N*) of 15 molecules (i.e, 855 atoms) contained into a cubic box with periodic boundary conditions (PBC). The side of the box was set to $L = 21.5$ Å for the calculations performed at 400 K in order to produce a density of 1 g/cm^3 at this temperature. The liquid was assumed to have a thermal expansion coefficient $\alpha = V^{-1}(\delta V/\delta T) \approx 10^{-3}$ K^{-1} and the side of the box was modified in accordance. Specifically, values of L = 21.85, 22.19, 22.84, and 23.76 Å were used respectively for temperatures of 450, 500, 600, and 750 K.

The energy of the single molecule was first minimized with respect to all internal coordinates, i.e., bond lengths, bond angles, and rotations. This optimized structure was employed as the starting conformation for all the MD simulations. The first part of every simulation consisted in warming up the sample from 0 K to the desired working temperature with increments of 50 K and allowing 10^4 fs for thermostation at every new temperature. Once the system was thermostated at the working temperature, the MD simulation was continued for 10^7 fs, recording the atomic coordinates every $\Delta = 50$ fs, thus producing a set of 2^5 conformations that were employed in the subsequent analysis.

The PBC system was initially built within a much larger box having $L_0 = 34.4$ Å, with one molecule placed at the center of the cube and the other 14 located close to the vertexes and centers of the faces, to avoid interpenetrations among different molecules which would produce unrealistically high values of energy, thus rendering difficult and unreliable any conceivable strategy for energy minimization. A MD simulation at high temperature (i.e., 1000 K) was then applied to this initial system with increments of −0.2 Å and allowing a relaxation time of 500 fs at each new size. Once the final volume was obtained, the system was cooled to 50 K, with increments of −50 K and allowing relaxation times of 500 fs at each new temperature. The energy of this structure was then minimized with respect to all internal coordinates to produce the optimized conformation

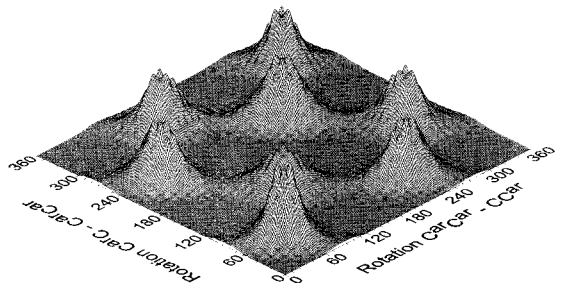

Figure 3. Distribution of probabilities for the rotational states of the C^{ar}-$C(CH_3)_2$−C^{ar} pair of bonds obtained from the MD simulation of the isolated molecule at 300 K.

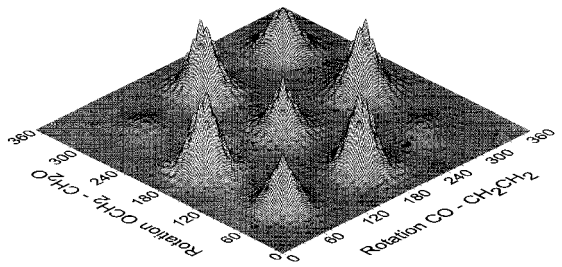

Figure 4. Distribution of probabilities for the rotational states of the CO−CH_2−CH_2O pair of bonds obtained from the MD simulation of the isolated molecule at 300 K.

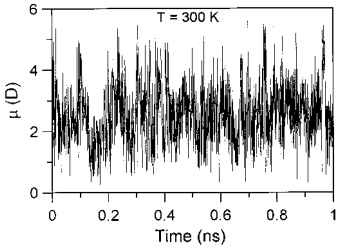

Figure 5. Dipole moments of the conformations adopted by the isolated molecule during the first nanosecond of MD simulation at 300 K. Values for the rest of the simulation are similar and are not shown in order to expand the time axis. Averaged values for the whole simulation are $\langle\mu\rangle = 2.61$ D and $\langle\mu^2\rangle = 7.90$ D^2.

that was employed as a starting point for the MD trajectories. Again, the first part of the simulations consisted in warming up the system from 0 K to the working temperature with increments of 50 K and relaxation periods of 500 fs at each new temperature. The data collection process consisted in 10^6 further steps (covering a total time span of 1 ns), recording the atomic positions every $\Delta = 50$ fs.

The time spans covered by the MD simulations (i.e., 10 ns for the isolated molecule and 1 ns for the molecular ensemble) are very large in order to ensure that the system will be able to statistically sample all the allowed conformational space. The quality of the sampling may be appreciated in Figures 3 and 4, which represent respectively the distribution of probabilities for the rotational states of the C^{ar}−$C(CH_3)_2$−C^{ar} and CO−CH_2−CH_2O pair of bonds obtained from the MD simulation of the isolated molecule at 300 K. Figure 5 shows the dipole moments of the conformations adopted by the isolated molecule during the first nanosecond of the MD simulation at 300 K. Values for the rest of the simulation are similar and are not shown in this figure in order to expand the time axis. Averaged values for the whole simulation are $\langle\mu\rangle = 2.61$ D and $\langle\mu^2\rangle = 7.90$ D^2, in excellent agreement with the experimental values.

Values of the dipolar auto-correlation coefficient $g(t)$ were computed at several temperatures as a function of time by means of the expresion:[22]

$$g(n\Delta) = \frac{1}{\langle\mu^2\rangle(N-n)}\left(\sum_{k=1}^{N-n}\mu[k\Delta]\mu[(k+n)\Delta]\right) \qquad (4)$$

where N is the total number of conformations recorded along the MD trajectory, $n = 0, 1, 2, \ldots$, and $\Delta = 50$ fs is the time gap between two consecutive conformations. In fact, this equation represents an average over the $N - n$ values of $g(t)$ obtained with all the pairs of conformations that are separated by a time equal to $n\Delta$. The value of the autocorrelation coefficient decreases rather fast with increasing time, thus $g(n\Delta) \approx 0$ for values of n which are much smaller than N and therefore $(N - n)$ is very large, which ensures a good sampling of $g(t)$ over all the conformational space.[22,23] The results of $g(t)$ obtained at several temperatures are shown in Figure 6 for the isolated molecule and in Figure 7 for the molecular ensemble. The values of $g(t)$ are well fitted by a Kohlrausch−Williams−Watts stretch exponential decay:[11−13]

$$g(t) = \exp\left[-\left(\frac{t}{\tau^*}\right)^{\bar{\beta}}\right] \qquad (5)$$

The values of the τ^* and $\bar{\beta}$ parameters that produce best fit to the results of $g(t)$ computed for both the isolated molecule and the molecular ensemble with PBC are summarized in Table 1. The results given in this table indicate that τ^* decreases with increasing temperature whereas $\bar{\beta}$ remains almost constant, i.e., $\beta \approx 0.50 \pm 0.05$ in most cases.

The mean-relaxation time of the system may be obtained by integration of $g(t)$ over time:

$$\tau = \int_0^\infty g(t)\,\mathrm{d}t \qquad (6)$$

The results obtained for both systems are shown as an Arrhenius plot, $\ln(\tau)$ vs $1/T$, in Figure 8. The values obtained for the isolated molecule are well fitted by a straight line with a slope of 1.4×10^3 K, which suggests an energy barrier of about 2.8 kcal/mol. The fitting is poorer in the case of the molecular ensemble, although the slope is also 1.4×10^3 K.

The normalized complex dielectric permittivity ϵ^* may be expressed as the Laplace transform of the derivative with respect to time of the time-dipole correlation function:[23−26]

$$\frac{\epsilon^*(\omega) - \epsilon_\infty}{\epsilon_0 - \epsilon_\infty} = \int_0^\infty\left[-\frac{\partial g(t)}{\partial t}\right]\mathrm{e}^{-i\omega t}\,\mathrm{d}t \qquad (7)$$

with ω being the angular frequency. Integration of this equation allows the evaluation of both the real ϵ' and loss ϵ'' components of ϵ^* as

$$\frac{\epsilon'(\omega) - \epsilon_\infty}{\epsilon_0 - \epsilon_\infty} = 1 - \omega\int_0^\infty g(t)\sin(\omega t)\,\mathrm{d}t$$

$$\frac{\epsilon''(\omega)}{\epsilon_0 - \epsilon_\infty} = \omega\int_0^\infty g(t)\cos(\omega t)\,\mathrm{d}t \qquad (8)$$

Values of the loss component ϵ'' calculated at several temperatures by direct integration of $g(t)$ computed from the MD trajectories of the isolated molecule are represented in Figure 9. The curves show that the maximum of ϵ" moves toward higher frequencies with increasing temperature and, at the same time, the relaxation becomes narrower. Similar

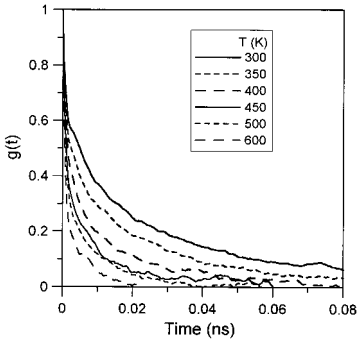

Figure 6. Values of the time dipole autocorrelation coefficient $g(t)$ obtained for the isolated molecule at several temperatures.

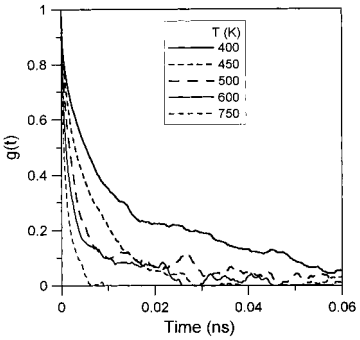

Figure 7. Values of the time dipole autocorrelation coefficient $g(t)$ obtained for the molecular ensemble at several temperatures.

TABLE 1: Values of the τ^* (in ps, i.e., 10^{-12} s) and β Parameters for the KWW Stretch Exponential Decay (Eq 5) That Produces Best Fit for the Time Dipole Autocorrelation Coefficient $g(t)$ of Both the Isolated Molecule and the Molecular Ensemble[a]

	eq 5			eq 6
T, K	τ^*, ps	β	$10^4\,\sigma^2$	τ, ps
		Isolated Molecule		
300	9.95	0.480	1.5	21.5
350	6.15	0.457	0.8	14.7
400	3.42	0.456	0.8	8.2
450	2.26	0.464	2.2	5.3
500	1.80	0.471	1.4	4.0
600	1.09	0.501	4.7	2.2
		Molecular Ensemble		
400	9.19	0.550	3.3	15.6
450	5.02	0.689	3.0	6.5
500	2.46	0.452	9.0	6.0
600	1.49	0.430	4.0	4.1
750	0.39	0.324	8.5	2.5

[a] The fourth column gives the values of the standard deviation of the fits. The last column indicates the relaxation times obtained from eq 6.

behavior is exhibited by the curves obtained from the simulations in the molecular ensemble.

Discussion

An inspection of the simulated trajectories permits one to conclude that at the lowest temperature employed in the present work, the isolated molecules visit all the configurational space in less than 0.1 ns. On the other hand, the fact that the mean-square dipole moment calculated from the trajectories is in very good agreement with the experimental result gives confidence to the distribution of charges used in the simulations.

The time dipole correlation coefficient calculated for both the isolated molecule and the molecules in the bulk fit

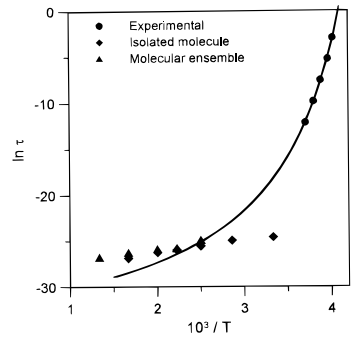

Figure 8. Arrhenius plot for the experimental and simulated results of the dielectric relaxation of 2,2-bis[4-(2-hydroxyethoxy)phenyl]-propane diacetate. The symbols (●), (♦), and (▲) represent, respectively, the relaxation times obtained from experiments and simulations for an isolated molecule and for a molecular ensemble. The continuous line corresponds to the VFTH equation fitting the experimental results.

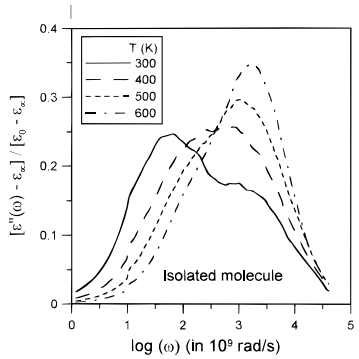

Figure 9. Normalized loss component of the complex dielectric permittivity $[\epsilon''(\omega) - \epsilon_\infty]/[\epsilon_0 - \epsilon_\infty]$ as a function of the angular frequency ω computed for the isolated molecule at several temperatures.

reasonably well to the KWW equation. This indicates that the response in the time domain obtained by simulation exhibits, like the glass−liquid relaxation, stretched behavior. However, important differences are observed in the temperature dependence of the relaxation times of the simulated relaxation response when compared with those corresponding to the experimental α relaxation. The Arrhenius plot of the mean relaxation times in Figure 8 shows, as usual, that the α relaxation fits to the VFTH equation, but this does not occurs with the values simulated for the relaxation times at temperatures well above the glass transition temperature. At these temperatures the DDA compound may be in the equilibrium liquid range and therefore the relaxation response to an external perturbation is the single $\alpha\beta$ absorption. However, whereas there is a wealth of information concerning the stretched behavior of the α relaxation, the information concerning the shape of the $\alpha\beta$ process is rather limited. The results at hand seem to suggest that the activation energy associated with the $\alpha\beta$ process, $E_{\alpha\beta}$, is significantly lower than that of the α relaxation and presumably is of the same order or lower than that of the β relaxation.[27]

A model has been formulated[12] that assumes that both liquids and supercooled liquids are formed, from a dynamic point of view, by heterogeneous cooperative and noncooperative regions. According to the model, the β relaxation originates from the relaxation of the fast relaxators in the noncooperative regions and it shows symmetric broadened behavior. The α relaxation arises from the relaxation of slow relaxators in the cooperative regions and it shows a broaden and skewing behavior. Finally, the $\alpha\beta$ relaxation originates either from the spatial energy coupled relaxation between the cooperative and noncooperative

regions or from the coupled relaxation of the fast relaxators. The model, which gives a good account of the relaxation of supercooled liquids and the glass transition, in a unified way, predicts the $\alpha\beta$ relaxation stretching behavior, as obtained in the simulation of the time dipole correlation function in this work.

A few comments should be made on the similarity of the responses simulated for isolate molecules and in the bulk. In both case the simulations show stretching behavior with rather low $\bar{\beta}$ exponents. The dipole correlation function in eq 2 includes autocorrelation and cross-correlation terms for the time dipole relaxation function. It is obvious that the cross-correlation terms in this equation will have appreciable magnitude and their signs may be positive or negative. However, it has been reasoned from theoretical considerations and experimental dielectric results for polar−nonpolar random copolymers that the autocorrelation and cross-correlation functions have the same time-dependence.[13] The same conclusion was obtained from MD simulations performed in other systems.[22] Accordingly, the cross-correlation terms, although present, do not significantly alter the time-dependence of $g(t)$ and therefore an understanding of the dielectric relaxations may be obtained from the autocorrelation function.[13]

Conclusions

The dielctric relaxation behavior of supercooled liquids can, in principle, be predicted by molecular dynamics simulation methods. However, the unreasonably large computing time involved in the simulations at temperatures near T_g restricts the simulations to temperatures well above the glass transition temperature. At these temperatures the relaxation response to perturbation fields exhibits a stretch behavior, like the α or glass−liquid relaxation, but the temperature dependence of its mean-relaxation time is rather small, in comparison with that of the α process. These results are in good agreement with the predictions of a model recently formulated that considers liquids and supercooled liquids, from a dynamic point of view, as formed by cooperative and noncooperative regions.

Acknowledgment. This work was supported by the DGICYT through Grant PB97-0778 and PB95-0134-C02-01.

References and Notes

(1) Angell, A. *Science **1995**, 267, 1615.*
(2) Stillinger, H. *Science* **1995**, *267*, 1935.
(3) Frick, B.; Ritcher, D. *Science* **1995**, *267*, 1939.
(4) Hodhe, M. *Science* **1995**, *267*, 1945.
(5) Greer, L. *Science* **1995**, *267*, 1947
(6) Jäckle, J. *Rep. Prog. Phys.* **1982**, *49*, 171.
(7) Vogel, H. *Z. Phys.* **1921**, *22*, 645.
(8) Fulcher, G. S. *J. Am. Ceram. Soc.* **1925**, *8*, 339.
(9) Tammann, G.; Hesse, W. *Z. Anorg. Allg. Chem.* **1926**, *156*, 245.
(10) Götze, W.; Sjögren, L. *Rep. Prog. Phys.* **1992**, *55*, 241.
(11) Williams, G.; Watts, D. *Trans. Faraday Soc.* **1970**, *66*, 80.,
(12) Huang, Y. N.; Wang, Y. N.; Riande, E. *J. Chem. Phys.* **1999**, *111*, 8503.
(13) Williams, G. *Dielectric Relaxation Spectroscopy of Amorphous Polymer Systems: The Modern Approaches*, in *Keynote Lectures in Polymer Science*; Riande, E., Ed.; CSIC: Madrid, 1995.
(14) Riande, E.; Díaz-Calleja, R.;.Guzmán, J. *J. Phys. Chem.* **1991**, *95*, 7104.
(15) Riande, E.; Saiz, E. *Dipole Moments and Birefringence of Polymers*; Prentice Hall: Englewood Cliffs, NJ, 1992.
(16) Allen, M. P.; Tildesley, D. J. *Computer Simulation of Liquids*; Claredon Press: Oxford, 1987.
(17) Forester, T. R. ; Smith, W. *DL_POLY* (Ver. 2.1), Daresbury Laboratory, Daresbury, Warrington WA4 4AD, England.
(18) Weiner, S. J.; Kollman, P. A.; Case, D. A.; Singh, U. C.; Ghio, C.; Alagona, G.; Profeta, S. Jr.; Weiner, P. *J. Am. Chem. Soc.* **1984**, *106*, 765.
(19) Weiner, S. J.; Kollman, P. A.; Nguyen, D. T.; Case, D. A. *J. Comput. Chem.* **1986**, *7*, 230.
(20) Homans, S. W. *Biochemistry*, **1990**, *29*, 9110.
(21) MOPAC, *Quantum Chemistry Program Exchange*, Department of Chemistry, Indiana University, Bloomington, IN.
(22) Saez-Torres, P.; Saiz, E.; Díaz-Calleja, R.; Guzmán, J.; Riande, E. *J. Phys. Chem. A* **1998**, *102*, 5763.
(23) Saiz, E.; Riande, E.; Díaz-Calleja, R. *J. Phys. Chem. A* **1997**, *101*, 7324.
(24) Williams, G.; Watts, D. C.; Dev, S. B.; North, A. M. *Trans. Faraday Soc.* **1971**, *67*, 1323.
(25) Riande, E.; Saiz, E. *Curr. Trends Polym. Sci.* **1997**, *2*, 1.
(26) Saiz, E.; Riande, E. *J. Non-Crystalline Solids* **1998**, *235−237*, 353.
(27) Garwe, F.; Schönhals, A.; Lockwenz, H.; et al. *Macromolecules* **1996**, *29*, 247.